Journal of Hazardous Materials

ELSEVIER

Characterization of the catalytic films formed on stainless steel anodes employed for the electrochemical treatment of cuprocyanide wastewaters

Lidia Szpyrkowicz[a,1], Francesco Ricci[a], M. Fátima Montemor[b,2], Ricardo M. Souto[c,*]

[a] *Environmental Sciences Department, University of Venice, 30123 Venice, Italy*
[b] *Chemical Engineering Department, Instituto Superior Técnico, 1096 Lisboa, Portugal*
[c] *Department of Physical Chemistry, University of La Laguna, 38071 La Laguna, Tenerife, Canary Islands, Spain*

Abstract

Surface composition changes at stainless steel anodes in an electrochemical reactor applied for the electrochemical treatment of cuprocyanide-containing wastewaters operating under different hydrodynamic conditions were investigated. Under highly alkaline conditions in situ generation of a surface film on the anode with catalytic properties towards cyanide electrolysis was observed. X-ray photoelectron spectroscopy (XPS) results demonstrated that only copper oxi-hydroxide compounds constitute the surface film developed on the stainless steel anodes, as no traces of N- and C-containing compounds were observed. The collected XPS spectra revealed relevant details concerning the oxidation states of copper in the film, and the products Cu_2O, CuO and $Cu(OH)_2$ were identified on the surface of the anodes. However, the quantitative proportions of the individual products differ and depend on the type of mixing employed during reactor operation.
© 2004 Elsevier B.V. All rights reserved.

1. Introduction

Cyanide bearing wastewaters are generated in electrolytic baths during metal deposition in general, and copper in particular. These wastewaters are environmentally hazardous and require detoxification operations before they are returned to the environment. Traditional treatment of these wastewaters consists in the chemical oxidation of the cyanide species and the simultaneous precipitation of the metal ions as hydroxides. Such procedures require the need for chemical additives and sludge disposal. An interesting alternative is provided by electrochemical oxidation methods [1–5], because they minimize the need for chemical additives and facilitate the recovery of metals through electrodeposition at the cathode of the electrochemical reactor.

Several electrode materials have been tested so far, though the electro-oxidation of complexed cyanides was observed to occur with a slower kinetics as compared to the electro-oxidation of free cyanide [6–11]. Higher electro-oxidation rates were also observed when copper was present in the medium. In this case, the formation of a surface film on the anode which exhibited electrocatalytic properties was observed [12–15]. The best performance for the destruction of free cyanides has been achieved in reactors equipped with platinum and platinum-modified anodes [16–19]. The elevated cost of these materials has imposed a new trend in the investigation directed to testing alternate materials for electrodes fabrication. In this respect, interesting results have been obtained at our laboratories in lab-scale batch electrochemical reactors equipped with stainless steel electrodes [20–23]

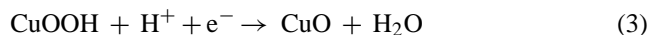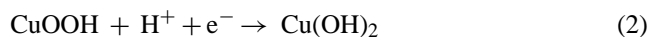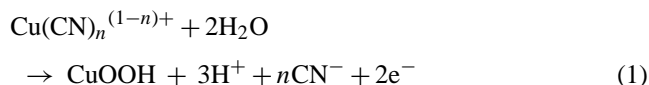* Corresponding author. Tel.: +34 922 318030; fax: +34 922 318002.
E-mail addresses: lidia@unive.it (L. Szpyrkowicz),
mfmontemor@alfa.ist.utl.pt (M.F. Montemor), rsouto@ull.es (R.M. Souto).
[1] Fax: +39 041 2348591.
[2] Fax: +351 21 8404589.

under controlled operation conditions which allow for the deposition on the anode of films which exhibit electrocatalytic properties. In this way, comparison of the efficiency of a reactor equipped with either a Ti/Pt or a plated stainless steel anode operating at an alkaline pH of 13 [19], proved the performance of the former to be only slightly better than the performance with the modified SS anode. Though the results of treatment depended to some extent on the anode material, the formation of the electrocatalytic film on the surface of the anodes mainly depended on the chemical, electrical and hydrodynamic conditions under which the electrochemical reactor operated (applied potential and current, chemical composition of the electrolytic solution and the hydrodynamic regimes in the reactor) [12,16–23]. It was demonstrated that the type of mixing and its intensity strongly affected the performance of the electrochemical reactor in terms of single pollutants: cyanides and copper, which correlated well with the extent of deposition for the electrocatalytic anodic film [22,23]. In situ formation of this film was achieved provided a minimum turbulence was imposed in the reactor. Too vigorous stirring, however, exerted a shear stress, exceeding which the removal of the film occurred [20,22]. In this way, the possibility to use cheaper materials for the construction of the electrodes such as stainless steel was demonstrated [19–23].

A mechanism accounting for the in-situ formation of an electrocatalytic film on the anode during the electrochemical oxidation of copper complex cyanide solutions under alkaline conditions has been proposed [24], which can be expressed in terms of the following sequence of reactions:

$$Cu(CN)_n^{(1-n)+} + 2H_2O$$
$$\rightarrow CuOOH + 3H^+ + nCN^- + 2e^- \tag{1}$$

$$CuOOH + H^+ + e^- \rightarrow Cu(OH)_2 \tag{2}$$

$$CuOOH + H^+ + e^- \rightarrow CuO + H_2O \tag{3}$$

On the other hand, copper electrodeposition simultaneously occurs on the cathode with liberation of CN^- ions according to [25]:

$$Cu(CN)_2^- + e^- \rightarrow Cu + 2CN^- \tag{4}$$

As the experimental objective of our previous studies was to define electrode surface reactions with electrochemical techniques (i.e., through the analysis of measurable parameters of current, electrode potential, and reactant concentration), the chemical characterization of the electrodeposited products on the electrode surface could not be attempted. This was hampered by the lack of molecular specificity in the electrochemical measurements. In addition, the electrocatalytic behaviour of electrode surfaces remained difficult to quantify with conventional electrochemical measurements. The application of surface analytical techniques such as X-ray photoelectron spectroscopy (XPS, also referred to as electron spectroscopy for chemical analysis) [26,27], which can yield molecular information relevant to the electrode surface chemistry, offer a new insight into these problems.

The main purpose of this work was to examine the composition and structure of the catalytic films formed on stainless steel anodes during the destruction of cuprocyanide species in aqueous solution under optimised hydrodynamic operating conditions [22]. A necessary minimum rate of mass transport corresponding to a minimum dissipated power in the reactor of $1.5 \, W/m^3$ was needed to form the electrocatalytic anodic film. However, too vigorous stirring caused shear-induced detachment of the film at shear stresses above $0.41 \, N/m^2$. Conversely, mechanical stirring was unsatisfactory as shear rates over the anode were non-uniformly distributed and instantaneous liquid velocities were subject to large fluctuations. After electrolysis, information on the morphology and composition of anode films was obtained by X-ray photoelectron spectroscopy and scanning electron microscopy (SEM).

2. Experimental

2.1. Preliminary cyclic voltammetry

To define the potential range at which the formation of the electrocatalytic film of copper oxides occurs, cyclic voltammograms were determined for 316 stainless steel plate placed in a flat-cell configuration exposing to the electrolyte a circular working area of $1 \, cm^2$. A saturated calomel electrode (SCE) was used as reference and a platinum gauze served as auxiliary electrode. The working electrolyte was a NaOH solution adjusted at pH 13.0. The investigated solutions contained either 5.05 g/l KCN or 3.5 g/l KCN + 2.14 g/l CuCN, allowing the total amount of cyanide species to be the same in both electrolytes. Cyclic voltammograms were recorded at a scan rate of 0.1 V/s using a 283A EG&G portentiostat–galvanostat. All measurements were performed at room temperature and the electrochemical cell was open to air.

2.2. Formation and characterization of electrocatalytic film

An undivided cell electrochemical reactor (0.15 m × 0.06 m × 0.205 m) made of glass, equipped with parallel plate type 316 stainless steel electrodes, was used to treat cyanide bearing wastewater under potentiostatic conditions and different stirring modalities and rates. A dc stabilised power source (DD Associates, India) was used to supply power at cell voltages of 1–10 V, while the anode potential was measured against a home-made saturated calomel reference electrode (*SCE*) placed in a Luggin capillary probe, using a high impedance voltmeter (Keithley 169 Multimeter). The electrochemical reactor was operated under isothermal conditions at the temperature of $20 \, °C$, using a Haake Nr 3 thermostatic bath. Exhaustive electrolysis was conducted using the synthetic wastewater, which contained 520 mg/l of CuCN and 94 mg/l of NaCN. The pH of the electrolyte was adjusted to 13.0 by dosing NaOH.

Two conditions of reactor operation were considered for this work, which corresponded to the optimum operation of the system under either gas mixing or hydraulic mixing [22]. Namely, gas sparging with air produced the best film in terms of uniformity and adherence, while pumping resulted in an acceptable film with the lowest energy consumption. In both cases, the electrochemical reactor operated at a constant current density of 2.3 A/dm^2 for 15 min. In these conditions, the anode experienced a potential of 1.0 V. The gas mixing was attained by introducing compressed air at the bottom of the reactor via a ceramic porous set at a flow rate of 2.2×10^{-2} l/s. Hydraulic mixing was achieved with a peristaltic pump (Watson Marlow Mod. 313 F/D), equipped with two heads, operating under conditions of a full recycle, at the flow rate of 880 ml/min.

After electrolysis, the film on the anode was analyzed by X-ray photoelectron spectroscopy and scanning electron microscopy. The XPS spectra were recorded on a VG Scientific MICROLAB 310F spectrometer equipped with a concentric hemispherical electron analyser and a Mg Kα X-ray excitation source ($h\nu = 1253.6$ eV). 20.40 eV energy regions of the photoelectrons of interest were scanned several times to obtain adequate signal-to-noise ratios. The photoelectron spectra corresponding to N-1s, O-1s, C-1s, Cu-2p, and Fe-3d signals were measured. Although sample charging was observed, accurate binding energies could be determined by referencing to the adventitious C-1s peak at 285.0 eV.

SEM micrographs of the electrocatalytic film formed on the anode were obtained by using a JEOL JSM-5310 equipment with an electron beam energy of 20 keV.

3. Results and discussion

3.1. Electrochemistry of cuprocyanide solutions at a stainless steel electrode

Before examining the composition and structure of the catalytic films formed on stainless steel anodes during the destruction of cuprocyanides species in aqueous solution, we present preliminary cyclic voltammograms describing the electrochemical behaviour of a stainless steel electrode immersed in the base electrolyte and in CN$^-$-containing solutions both in the absence and in the presence of copper species. The cyclic voltammogram measured in the base NaOH solution of pH 13.0 shows a sudden increase of the measured current in the positive-going potential scan at ca. 0.50 V, which is a consequence of the evolution of oxygen (see Fig. 1, dotted line). The addition of KCN to the base electrolyte gives rise to somewhat higher currents at potentials more positive than 0.50 V due to the contribution of a new oxidation process (cf. Fig. 1, dashed line), which results from the direct oxidation of CN$^-$ through a mechanism of the type [28,29]:
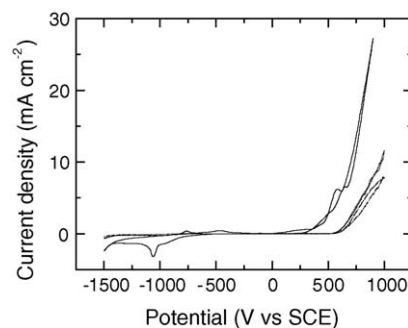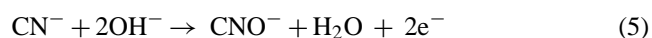
$$CN^- + 2OH^- \rightarrow CNO^- + H_2O + 2e^- \tag{5}$$

Fig. 1. Cyclic voltammograms for a 316 stainless steel electrode in NaOH aqueous solutions adjusted at pH 13.0. (·····) base electrolyte; (- - - - -) base electrolyte + 5.05 g/l KCN; and (—) base electrolyte + 3.5 g/l KCN + 2.14 g/l CuCN. Scan rate: 0.1 V/s.

When the cyanides are present as copper complexes, the measured cyclic voltammogram exhibits significant new features, as it can be observed from the inspection of the typical voltammogram depicted as a full line in Fig. 1. In the CuCN-containing solution, during the run of potential in the positive direction, two voltammetric peaks can be observed in the $-0.7 < E < -0.5$ V potential range, which result from the onset of copper oxide formation with oxidation states +1 and +2, respectively. Further increase of the potential leads to the observation of a major increase of current for $E > 0.45$ V to reach a well-defined voltammetric peak at ca. 0.58 V. After potential reversal at the switching anodic potential, a current crossover is observed during the negative-going potential scan, which is an indication of a complex electrochemical process, comprising both the oxidation of copper that continues occurring during the reverse scan within this potential range, with the formation of a new surface film, and the electro-oxidation of cyanides. Significantly higher oxidation currents are measured in the cuprocyanide solution as compared to the copper-free solution despite the total concentration of cyanide species was maintained constant in both electrolytes.

3.2. XPS investigation of anode surface films formed in an electrochemical reactor

XPS analysis has been used to determine the chemical nature of the catalytic films formed on the stainless steel anodes during the operation of the electrochemical reactor.

3.2.1. Characterization of copper standards

For the chemical identification of copper surface species, analysis of Cu-2p bands was performed. Copper standards covering the various oxidation states of copper that could be expected to be present on the anodes, were carefully prepared, and the corresponding XPS spectra were measured.

The XPS lines corresponding to pure metallic copper were determined from an electrolytic copper plate of 99.9% purity. The plate was mechanically polished until mirror-like brightness, degreased by rinsing with acetone, and subsequently introduced in the analyser chamber. Firstly, the survey spec-

trum was obtained, which served to confirm the absence of any spurious elements apart from the adventitious carbon signal resulting from surface contamination. The corresponding Cu-2p$_{3/2}$ signal is given in Fig. 2a. One peak was found around 933.9 eV. This value is too high for metallic copper and rather corresponds to the energies measured for CuO [27], thus indicating that some oxidation of the surface occurred during the pretreatment process. In order to minimize the effect of surface contamination, the specimen introduced in the analyzer chamber was also subjected to ion bombardment with Ar$^+$ ions for 20 s. This operation was performed at an argon pressure of 5.0×10^{-6} Torr and under an applied voltage of 3 kV. This operation resulted in the removal of a few layers of copper atoms from the surface of the specimen together with the surface contamination due to air exposure of the sample. This procedure produces a major decrease in the height of the C-1s signal, and a 1 eV shift of the Cu-2p signal (cf. dotted line in Fig. 2a). The resulting peak agrees well with the data recorded in the literature for Cu(0).

Next, the XPS spectra of a copper(II) blank were measured. The CuO specimen was obtained by the thermal decomposition of hydrated copper sulphate under an oxidating atmosphere according to:

$$CuSO_4 \cdot 5H_2O \rightarrow CuO + SO_2 + H_2O \qquad (6)$$
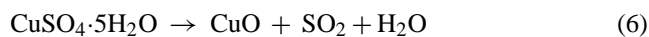
The resulting oxide compound exhibited a dark brownish colour, and was introduced inside a dissicator to avoid its
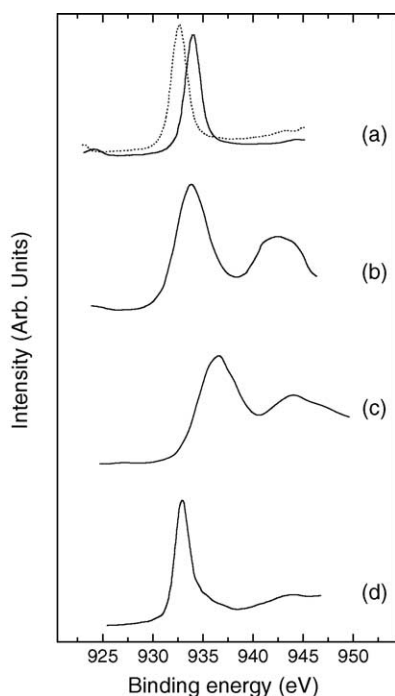

Fig. 2. Cu-2p$_{3/2}$ XPS spectra for different copper standards. (a) Cu(0) specimen: the continuous line corresponds to the spectrum obtained after introduction of the specimen in the instrument, and the dotted line depicts the spectrum measured after sputter cleaning by Ar$^+$ ions; (b) CuO sample; (c) CuO–Cu(OH)$_2$ sample and (d) Cu$_2$O sample.

rehydration prior to the measurement of the corresponding XPS spectra. Analogously to the previous case, after the specimen was introduced in the analyzer chamber and the corresponding survey spectrum was obtained, the signal for Cu-2p was recorded. The resulting spectrum is presented in Fig. 2b. The presence of Cu^{+2} in CuO is characterized by a high-intensity shake-up satellite which appears at ca. 10 eV higher binding energy than the main Cu-2p$_{3/2}$ peak, and is considerably broader than in the case of Cu metal (cf. spectra b and a in Fig. 2) [30–34].

In order to test the possible occurrence of hydroxide formation in addition to copper(II) oxide formation in the electrocatalytic films formed on steel, a high-purity electrolytic copper plate was electro-oxidized up to 0.65 V in an aqueous solution containing 0.1 M Na$_2$CO$_3$, according to the procedure described in references [34,35]. In this case, the XPS spectrum measured in Cu-2p$_{3/2}$ region for the Cu^{+2} surface is drawn in Fig. 2c. Direct comparison of this spectrum with that in Fig. 2b allows to observe that both the main peak and the satellite characteristic of the oxidation state +2 of copper are broaden, by covering higher binding energies. This is due to the occurrence of copper(II)-hydroxide in addition to CuO [35,36].

Finally, the XPS spectra characteristic of the oxidation state +1 of copper were obtained after the electrochemical preparation of Cu$_2$O in an aqueous containing 0.1 M Na$_2$CO$_3$ solution at −0.34 V [34,37]. The XPS spectrum measured in Cu-2p$_{3/2}$ region for the Cu$_2$O specimen is drawn in Fig. 2d. No shake-up satellite is observed this time (cf. Fig. 2b) [34,38,39].

3.2.2. Characterization of the anodes

The XPS spectra were also measured for the films formed on the stainless steel anodes after electrochemical treatment in the solutions containing cuprocyanide species. In this case, the anodes obtained under two selected hydrodynamic conditions in the cell were considered. Preparation conditions were selected on the basis of optimum current efficiency towards cyanide removal under both hydraulic and gas mixing given in ref. [22].

The formation of a greenish black deposit on the stainless steel anodes was observed during the electrolysis in the reactor, as depicted in Fig. 3. After electrolysis, surface analysis was performed by cutting 1 cm^2 plates from the anodes, which could be introduced in the spectrometer chamber.

Firstly, it was observed that the XPS spectra do not show the uptake of the organic ligand as no N-1s and C-1s signals could be observed above the background signal apart from the adventitious carbon signal for all the specimens tested. Secondly, analysis of the Cu-2p bands in both cases was consistent with the presence of copper species bearing oxidation states +1 and +2 on the surface of the stainless steel, as the corresponding contributions could be deconvoluted from the spectra in Fig. 4. No evidence for metallic copper deposition on the anode could be found.
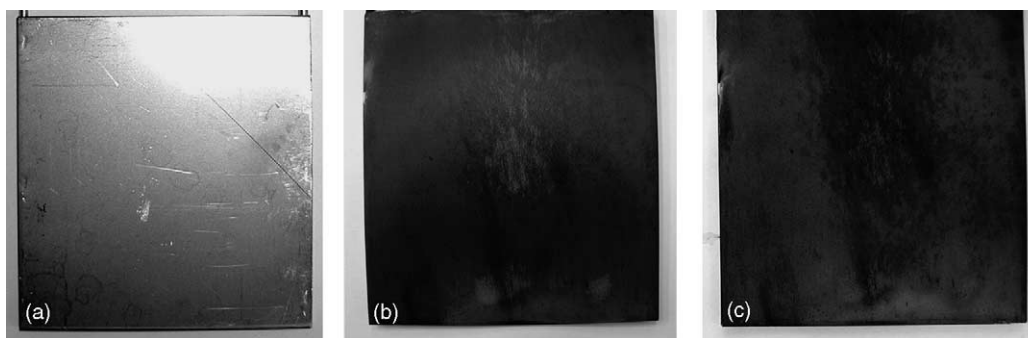
Fig. 3. Images of the stainless steel anodes used in this work: (a) prior to electrolysis; (b) after 15 min operation under air sparging and (c) after 15 min operation under hydraulic mixing. Electrolysis conditions are given in the text.
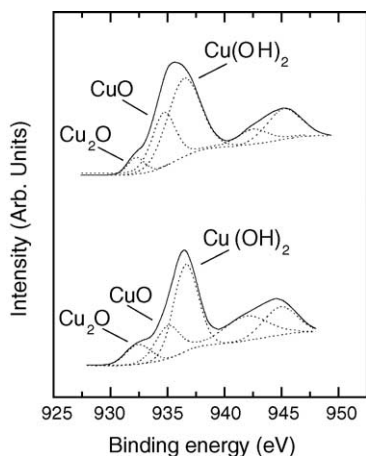

Fig. 4. Resolution of Cu-2p$_{3/2}$ XPS bands measured at stainless steel anodes after operation in cuprocyanide solution under: (a) air sparging and (b) hydraulic mixing. Electrolysis conditions are given in the text.

From the study of the Cu-2p$_{3/2}$ bands, one can observe the contributions due to cuprous and cupric oxides, and cupric hydroxide as labelled in the figure for the corresponded deconvoluted spectra. The existence of both oxide and hydroxides is confirmed from the analysis of the O-1s band (cf. Fig. 5), which is consistent with oxygen atoms distributed between two different chemical environments.

Furthermore, by a careful analysis of the Cu-2p$_{3/2}$ bands, the relative amount of each compound could be estimated, and the results are given in Table 1. The Cu^{II}/Cu^{I} ratio is observed to significantly depend on the preparation conditions of the anodes. In fact, this ratio is higher for gas sparging as compared to pumping, and the percentage of Cu$_2$O in the film in the case of the specimen treated under hydraulic operation is twice that measured from the specimen prepared under

Table 1
Distribution of compounds obtained from the deconvolution of the Cu-2p$_{3/2}$ XPS bands shown in Figs. 4 and 5

	Cu$_2$O (%)	CuO (%)	Cu(OH)$_2$ (%)
Pumping	14.1	24.0	61.9
Air sparging	7.3	29.3	63.4
Air sparging (thin)	14.2	34.4	51.4

gas mixing. Since the thickness of both catalytic films were observed to be the same within experimental error (namely, $59 \pm 1\ \mu m$ and $58 \pm 2\ \mu m$, for gas sparging and pumping, respectively), the results demonstrate the oxidating effect of atmospheric oxygen on Cu$_2$O, which results in the subsequent enrichment in Cu^{II} species of the catalytic film formed under gas sparging.

Direct information regarding the morphology of the anodes coated by the catalytic film was obtained by scanning electron microscopy. The specimens considered for characterization were obtained from the same anodes considered for the XPS analysis. SEM micrographs obtained from the anodes produced under gas mixing are presented in Fig. 6. They show the surface oxide film to appear as deposits on the surface, which offer a high roughness under a higher magnification. In this way, a highly porous film is attained. Observation of the anode surface in those areas that exhibited a lower coverage by the catalytic film of the stainless steel material, show the same features when observed under the scanning electron microscope.

Direct comparison of the micrographs obtained from each specimen shows that the surface appearance of the two films is different as observed by SEM. The specimens produced
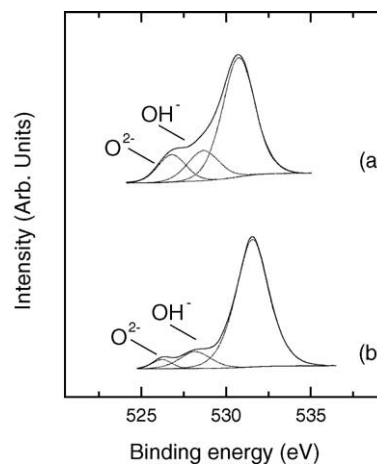

Fig. 5. Resolution of O-1s XPS bands measured at stainless steel anodes after operation in cuprocyanide solution under: (a) air sparging and (b) hydraulic mixing. Electrolysis conditions are given in the text.
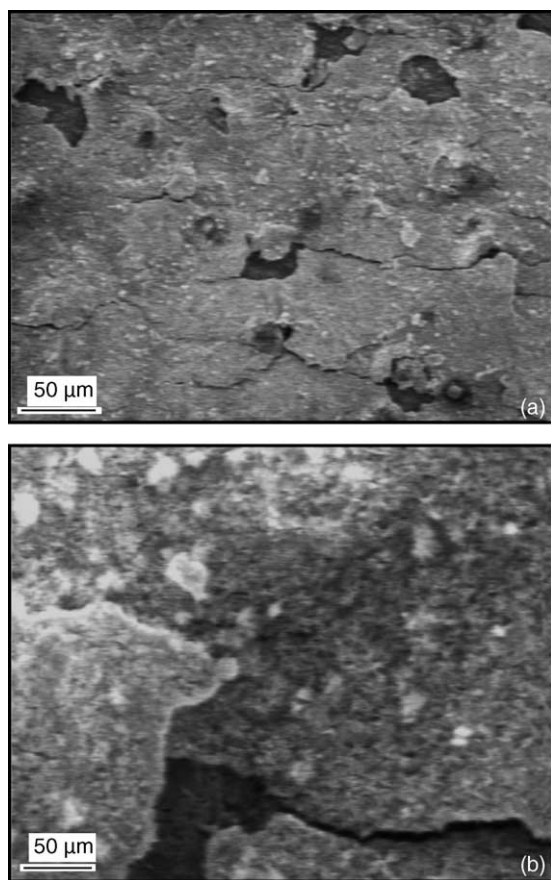
Fig. 6. SEM micrographs of a stainless steel anode after operation in cupro-cyanide solution under air sparging.

Fig. 7. SEM micrographs of a stainless steel anode after operation in cupro-cyanide solution under hydraulic mixing.

under hydraulic mixing (cf. Fig. 7) exhibit in addition to a deposit, which resembles quite closely that observed in the previous case, the formation of isolated clusters which are distributed randomly on the surface of the anode can be seen (see Fig. 7c). These deposits result in the formation of a surface of high roughness, thus offering a high-specific surface to the solution.

As observed through SEM microphotographs, hydrodynamic conditions operating in the electrochemical reactor do not result in the achievement of a homogeneous coverage of the anodes by the electrocatalytic film (cf. [22]). In fact, some areas show a thinner deposit compared to the average behaviour on the surface. In this case, the XPS spectra were also determined in those areas with a thinner film, as it is given in Fig. 8 in the case of gas mixing. The presence of both Cu^I and Cu^{II} oxi-hydroxides is observed again. But, deconvolution of the XPS spectrum shows that the areas with a thinner deposit are enriched in Cu_2O (see Table 1). This is a strong evidence to consider that a duplex oxide film is formed on the anode surface, in which the Cu^I-oxide forms the inner layer, whereas the Cu^{II}-oxide and the Cu^{II}-hydroxide constitute the outer layer. That is, Cu_2O constitutes the interface to the underlying stainless steel material.
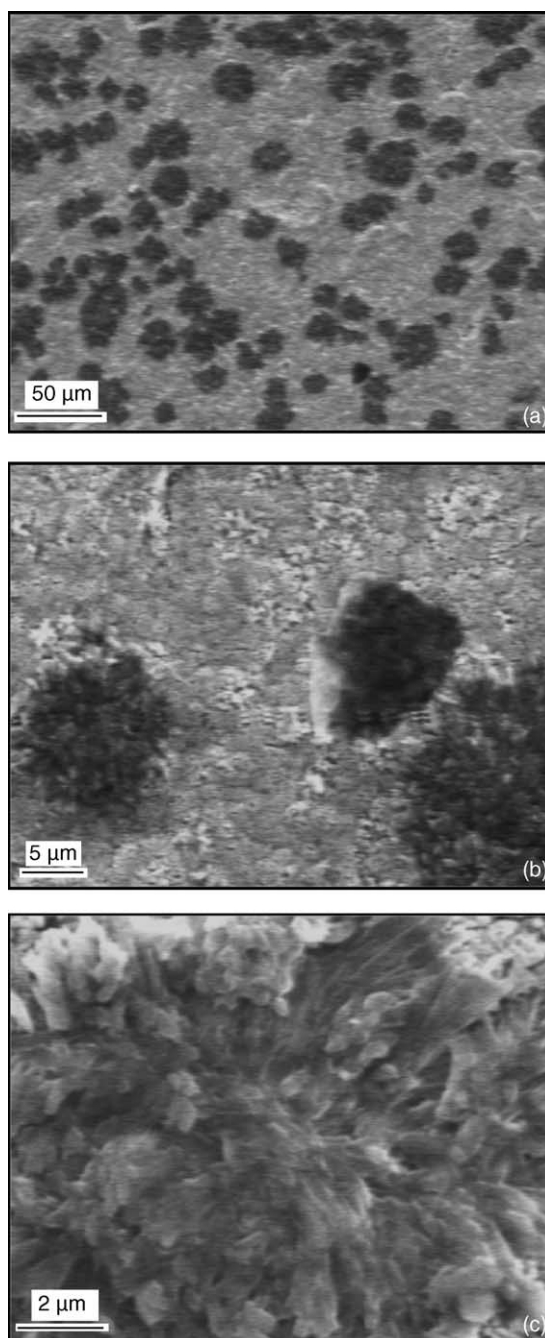
Finally, it should be noticed that bands originating from the underlying steel substrate contributed to the survey XPS spectra of the specimens too, as depicted in the typical example depicted in Fig. 9. A distribution of iron oxides and hydroxides are also observed in this case. Thus, the electrocatalytic film of copper oxihydroxides with a duplex structure seems to be built on top of an iron oxihydroxide layer in a similar manner as it forms on copper during the electro-oxidation of this metal in alkaline solutions [34,37,40].
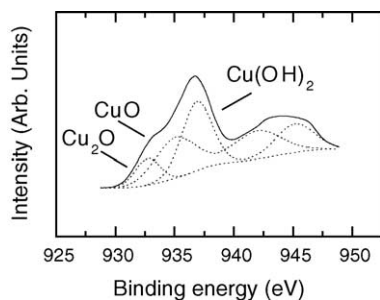
Fig. 8. Resolution of Cu-2p$_{3/2}$ XPS band measured in a zone where a thinner deposit of the catalytic film could be observed with the naked eye. The stainless steel anode was operated in cuprocyanide solution under air sparging.
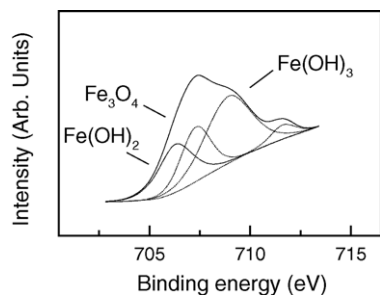

Fig. 9. Resolution of Fe-2p$_{1/2}$ XPS band of a stainless steel anode after operation in cuprocyanide solution under air sparging. Electrolysis conditions are given in the text.

4. Conclusions

This investigation was primarily designed to establish the effect of hydrodynamic regimes on the development of surface films on the stainless steel anodes employed in electrochemical reactors for the recovery of cuprocyanide wastewaters. These surface films are responsible for a significant electrocatalytic effect towards the oxidation of copper-cyanide complexes thus rendering a more economic and feasible electrochemical reactor for environmental applications.

Surface chemical analysis was firstly performed to investigate the applicability of the XPS technique for the assessment of the chemical composition of the surface films formed on the anodes. Secondly, surface chemical analysis was performed at a rather qualitative level for exploring any possible variation in the chemical data of the species present in the anodic surface film as a result of variations in the operating hydrodynamic conditions. However, the data available at this stage are scarce for attempting a mechanistic description of the electrochemical processes occurring on the anodes.

The applicability of XPS analysis for the study of this system has been demonstrated. Furthermore, the previous finding of strong effects of operating hydrodynamic conditions in the electrochemical reactor towards current efficiency and energy consumption for the process [23], can now be related to variations in the distribution of chemical species in the catalytic surface films formed on the anodes.

That is, the electrocatalytic films formed on the anodes operating under the optimum hydrodynamic conditions for various agitation types previously determined [22] have been investigated. Hydraulic stirring promotes copper electrode-position to a greater extent than mixing by compressed air, the later leading to slightly higher rates of cyanides removal. Though the greenish black deposits developed on the anodes are exclusively composed of cuprous and cupric oxide, it has been demonstrated that their relative distribution in the films depends on the mixing modes imposed in the electrochemical reactor. Therefore, it can be concluded that the differences in the chemical composition and the structure of the electrocatalytic films formed under different mixing regimes account for the observed differences in catalytic efficiency towards the removal of contaminants in diluted wastewater.

Finally, XPS data also demonstrate that there is no uptake of the cyanide species in the surface films, neither copper metal is deposited at the anodes.

Acknowledgements

References

[1] T.C. Tan, W.K. Teo, D.T. Chin, Electrochemical destruction of complex cyanide, Chem. Eng. Commun. 38 (1985) 125.

[2] S.P. Ho, Y.Y. Wang, C.C. Wan, Electrolytic decomposition of cyanide effluent with an electrochemical reactor packed with stainless-steel fiber, Water Res. 24 (1990) 1317.

[3] H. Bergmann, H. Hertwig, F. Nieber, Experimental and theoretical-studies on a new type of electrochemical reactor for waste-water treatment, Chem. Eng. Process. 31 (1992) 195.

[4] A. Buso, M. Giomo, L. Boaretto, G. Sandoná, A. Paratella, New electrochemical reactor for wastewater treatment: electrochemical characterisation, Chem. Eng. Process. 36 (1997) 255.

[5] A. Buso, M. Giomo, L. Boaretto, A. Paratella, New electrochemical reactor for wastewater treatment: mathematical model, Chem. Eng. Process. 36 (1997) 411.

[6] Ü. Bakir Ögütveren, E. Törü, S. Koparal, Removal of cyanide by anodic oxidation for wastewater treatment, Water Res. 33 (1999) 1851.

[7] H. Tamura, T. Arikado, H. Yoneyama, Y. Matsuda, Anodic-oxidation of potassium cyanide on platinum-electrode, Electrochim. Acta 19 (1974) 273.

[8] T. Arikado, C. Iwakura, H. Yoneyama, H. Tamura, Anodic-oxidation of potassium cyanide on graphite electrode, Electrochim. Acta 21 (1976) 1021.

[9] E.A. El-Ghaoui, R.E.W. Jansson, C. Moreland, Application of the trickle tower to problems of pollution-control. II. The direct and indirect oxidation of cyanide, J. Appl. Electrochem. 12 (1982) 69.

[10] F. Hine, M. Yasuda, T. Iida, Y. Ogata, On the oxidation of cyanide solutions with lead dioxide coated anode, Electrochim. Acta 31 (1986) 1389.

[11] G.H. Kelsall, S. Savage, D. Brandt, Cyanide oxidation at nickel anodes. II. Voltammetry and coulometry of Ni/CN–H$_2$O systems, J. Electrochem. Soc. 138 (1991) 117.

[12] J.-Y. Hwang, Y.-Y. Wang, C.-C. Wan, Electrolytic oxidation of cuprocyanide electroplating waste-waters under different pH conditions, J. Appl. Electrochem. 17 (1987) 684.

[13] C.S. Hofseth, T.W. Chapman, Indirect electrochemical processes at a rotating-disk electrode—catalytic alkaline cyanide oxidation, J. Electrochem. Soc. 139 (1992) 2525.

[14] B. Wels, D.C. Johnson, Electrocatalysis of anodic oxygen-transfer reactions—oxidation of cyanide at electrodeposited copper-oxide electrodes in alkaline media, J. Electrochem. Soc. 137 (1990) 2785.

[15] C.S. Hofseth, T.W. Chapman, Electrochemical destruction of dilute cyanide by copper-catalyzed oxidation in a flow-through porous electrode, J. Electrochem. Soc. 146 (1999) 199.

[16] M.-L. Lin, Y.-Y. Wang, C.-C. Wan, A comparative-study of electrochemical reactor configurations for the decomposition of copper cyanide effluent, J. Appl. Electrochem. 22 (1992) 1197.

[17] L. Szpyrkowicz, J. Naumczyk, F. Zilio-Grandi, Electrochemical treatment of tannery waste-water using Ti/Pt and Ti/Pt/Ir electrodes, Water Res. 29 (1995) 517.

[18] L. Szpyrkowicz, F. Zilio-Grandi, S.N. Kaul, A.M. Polcaro, Copper electrodeposition and oxidation of complex cyanide from wastewater in an electrochemical reactor with a Ti/Pt anode, Ind. Eng. Chem. Res. 39 (2000) 2132.

[19] L. Szpyrkowicz, S.N. Kaul, E. Molga, M. DeFaveri, Comparison of the performance of a reactor equipped with a Ti/Pt and an SS anode for simultaneous cyanide removal and copper recovery, Electrochim. Acta 46 (2000) 381.

[20] L. Szpyrkowicz, F. Zilio-Grandi, S.N. Kaul, S. Rigoni-Stern, Electrochemical treatment of copper cyanide wastewaters using stainless steel electrodes, Water Sci. Technol. 38 (1998) 268.

[21] L. Szpyrkowicz, R.M. Souto, F. Ricci, S.N. Kaul, Simultaneous removal of cyanides and copper in an electrochemical reactor—effects of agitation, in: G.H. Kelsall, R. Woods (Eds.), Electrochemistry in Mineral and Metal Processing, Vol. 6, The Electrochemical Society, Pennington, 2003, p. 316.

[22] L. Szpyrkowicz, G.H. Kelsall, R.M. Souto, F. Ricci, S.N. Kaul, Hydrodynamic effects on the performance of an electrochemical reactor for destruction of copper cyanide. Part 1: in situ formation of the electrocatalytic film, Chem. Eng. Sci. 60 (2005) 523.

[23] L. Szpyrkowicz, G.H. Kelsall, R.M. Souto, F. Ricci, S.N. Kaul, Hydrodynamic effects on the performance of an electrochemical reactor for destruction of copper cyanide. Part 2—reactor kinetics and current efficiencies, Chem. Eng. Sci. 60 (2005) 535.

[24] I.G. Casella, M. Gatta, Anodic electrodeposition of copper oxide/hydroxide films by alkaline solutions containing cuprous cyanide ions, J. Electroanal. Chem. 494 (2000) 12.

[25] A. Katagiri, H. Inoue, N. Ogure, Cathodic polarization of copper electrode in CuCN–KCN solutions and the current distribution for copper deposition on grooved substrates, J. Appl. Electrochem. 27 (1997) 529.

[26] J.S. Hammond, N. Winograd, Electron spectroscopy for chemical analysis (ESCA) and electrode surface chemistry, in: R.E. White, J.O'M. Bockris, B.E. Conway, E. Yeager (Eds.), Comprehensive Treatise of Electrochemistry, Vol. 8, Plenum Press, New York, 1984, p. 445.

[27] D. Briggs, M.P. Seah (Eds.), Practical Surface Analysis, Vol. 1: Auger and X-ray Photoelectron Spectroscopy, John Wiley, New York, 1990.

[28] D.T. Sawyer, R.J. Day, Electrochemical oxidation of cyanide ion at platinum electrodes, J. Electroanal. Chem. 5 (1963) 195.

[29] A.T. Kuhn, The role of electrochemistry in environmental control, in: J.O'M. Bockris, B.E. Conway (Eds.), Modern Aspects of Electrochemistry, Vol. 8, Butterworths, London, 1973, p. 273.

[30] K.S. Kim, Charge-transfer transition accompanying X-ray photoionization in transition-metal compounds, J. Electron Spectrosc. Relat. Phenom. 3 (1974) 217.

[31] C. Benndorf, H. Caus, B. Egert, H. Seidel, F. Theime, Identification of Cu(I) and Cu(II) oxides by electron spectroscopic methods—AES, ELS and UPS investigations, J. Electron Spectrosc. Relat. Phenom. 19 (1980) 77.

[32] H.-H. Strehblow, B. Titze, The investigation of the passive behavior of copper in weakly acid and alkaline-solutions and the examination of the passive film by ESCA and ISS, Electrochim. Acta 25 (1980) 839.

[33] R.M. Souto, V. Fox, M.M. Laz, M. Pérez, S. González, Some experiments regarding the corrosion inhibition of copper by benzotriazole and potassium ethyl xanthate, J. Electroanal. Chem. 411 (1996) 161.

[34] S. González, M. Pérez, M. Barrera, A.R. González-Elipe, R.M. Souto, Mechanism of copper passivation in aqueous sodium carbonate–bicarbonate solution derived from combined X-ray photoelectron spectroscopic and electrochemical data, J. Phys. Chem. B 102 (1998) 5483.

[35] N.S. McIntyre, M.G. Cook, X-ray photoelectron studies on some oxides and hydroxides of cobalt, nickel and copper, Anal. Chem. 47 (1975) 2208.

[36] D.W. Shoesmith, S. Sunder, M.G. Bailey, G.J. Wallace, F.W. Stanchell, Anodic oxidation of copper in alkaline solutions. Part IV. Nature of the passivating film, J. Electroanal. Chem. 143 (1983) 153.

[37] M. Pérez Sánchez, R.M. Souto, M. Barrera, S. González, R.C. Salvarezza, A.J. Arvia, A mechanistic approach to the electroformation of anodic layers on copper and their electroreduction in aqueous solutions containing NaHCO$_3$ and Na$_2$CO$_3$, Electrochim. Acta 38 (1993) 703.

[38] U. Collisi, H.-H. Strehblow, The formation of Cu$_2$O layers on Cu and their electrochemical and photoelectrochemical properties, J. Electroanal. Chem. 284 (1990) 385.

[39] R.M. Souto, M.M. Laz, S. González, X-ray photoelectron spectroscopy and electrochemical studies on the interaction of potassium ethyl xanthate with metallic copper, J. Phys. Chem. B 101 (1997) 508.

[40] J. Gómez Becerra, R.C. Salvarezza, A.J. Arvia, The influence of slow Cu(OH)$_2$ phase formation on the electrochemical behaviour of copper in alkaline solutions, Electrochim. Acta 33 (1988) 613.